

# Flavour-Changing Neutral Scalar Interactions of the Top Quark

Nuno Filipe Castro <sup>1</sup>  and Kirill Skovpen <sup>2,\*</sup> 

<sup>1</sup> Laboratório de Instrumentação e Física Experimental de Partículas (LIP), Departamento de Física, Escola de Ciências, Universidade do Minho, 4710-057 Braga, Portugal

<sup>2</sup> Department of Physics and Astronomy, Faculty of Sciences, Ghent University, Sint-Pietersnieuwstraat 33, 9000 Gent, Belgium

\* Correspondence: kirill.skovpen@cern.ch

**Abstract:** A study of the top-quark interactions via flavour-changing neutral current (FCNC) processes provides an intriguing connection between the heaviest elementary particle of the standard model (SM) of particle physics and the new scalar bosons that are predicted in several notable SM extensions. The production cross sections of the processes with top-scalar FCNC interactions can be significantly enhanced to the observable level at the CERN Large Hadron Collider. The present review summarises the latest experimental results on the study of the top-quark interactions with the Higgs boson via an FCNC and describes several promising directions to look for new scalar particles.

**Keywords:** top quark; FCNC; Higgs boson; scalar; LHC; new physics

## 1. Introduction

Conservation laws and flavour-symmetry structures represent the core element of any theoretical model that provides a description of interactions involving elementary particles. An experimental study of fundamental interactions is an excellent probe of higher-order symmetries, potentially leading to the construction of a more complete model of nature, resolving the remaining unanswered questions of the remarkably successful standard model (SM). Flavour-violating processes in the quark sector in the electroweak interactions are allowed through the charged weak currents. Such flavour-changing transitions proceed via an exchange of a W boson between the two fermionic states. The weak eigenstates are treated as left-handed doublets, allowing transitions between the up- and down-type quarks, while the mass eigenstates are represented by a superposition of weak eigenstates connected via a unitary matrix. The rotation from one type of state to another is then expressed as the Cabibbo–Kobayashi–Maskawa (CKM) matrix which governs the flavour-mixing processes through the flavour-changing charged weak transitions [1]. The processes, where a fermion changes its flavour via an exchange of a neutral boson, are therefore absent at the tree level in the SM due to the unitarity of the rotational matrices and are called the flavour-changing neutral currents (FCNC) [2].

The effect of flavour mixing in the quark sector was first introduced using a three-quark model that only included the u, d, and s quarks [3]. The experimental studies of the  $K_L \rightarrow \mu^+ \mu^-$  decays and neutral kaon-mixing processes, however, indicated important difficulties in satisfying the theoretical predictions for the FCNC transitions [4]. The problem was theoretically solved in the 1970s by introducing the fourth type of quark, the charm (c) quark, in order to restore the quark–lepton symmetry of the weak interaction. It was shown that an additional contribution associated with an exchange of a c quark at the one-loop level almost completely cancels the respective contributions connected to the lighter quarks. This effect leads to a significant suppression of FCNC transitions at higher orders—the Glashow–Iliopoulos–Maiani (GIM) mechanism. The discovery of the c quark, just a few years later, confirmed these theoretical speculations [5,6]. The four-quark model was later extended to include five quark flavours, after the discovery of the bottom (b)



**Citation:** Castro, N.F.; Skovpen, K. Flavour-Changing Neutral Scalar Interactions of the Top Quark. *Universe* **2022**, *8*, 609. <https://doi.org/10.3390/universe8110609>

Academic Editors: Efe Yazgan and Suyong Choi

Received: 18 October 2022

Accepted: 16 November 2022

Published: 21 November 2022

**Publisher's Note:** MDPI stays neutral with regard to jurisdictional claims in published maps and institutional affiliations.



**Copyright:** © 2022 by the authors. Licensee MDPI, Basel, Switzerland. This article is an open access article distributed under the terms and conditions of the Creative Commons Attribution (CC BY) license (<https://creativecommons.org/licenses/by/4.0/>).

quark [7]. It took a bit longer for the top (t) quark to be experimentally observed in 1995, completing the SM to contain six quark flavours [8,9]. In a full representation of the quark sector, the tree-level transitions between different quark flavours are only allowed through the weak flavour-changing charged interaction, while the tree-level FCNC transitions are completely missing in the SM and are only possible as loop corrections.

The FCNC effects are predicted in the leptonic sector as lepton flavour-violating transitions. However, the branching fraction of such processes is expected at the level of  $\simeq 10^{-54}$ , in the case of the  $\mu \rightarrow e\gamma$  decay, due to an extreme suppression from the neutrino mass difference to the power of four, and is experimentally inaccessible [10–12]. The FCNC transitions in the decays of the hadronic states with s, c, or b quarks are observed experimentally [13–18]. The studies of these processes are, however, affected by the large uncertainties in the theoretical calculations of the branching ratios of the hadron decays, mainly driven by the non-perturbative long-distance strong interaction contributions.

The lifetime of the top quark ( $\tau_t \simeq 5 \times 10^{-25}$  s), which is shorter than the typical formation time of the bound states ( $\tau_{\text{had}} = 1/\Lambda_{\text{QCD}} \simeq 10^{-24}$  s), makes the processes with the top-quark production an excellent probe to search for FCNC effects. The absence of hadronic activity leading to the formation of bound states involving top quarks makes the study of the FCNC processes less affected by radiative QCD corrections. The FCNC effects can be probed in the top-quark production processes, as well as in the decays of the top quarks. The amplitude of an FCNC transition is proportional to the squared mass of the quark involved in the loop diagram. A remarkable suppression of the top-quark FCNC decays is explained by the fact that the only possible one-loop contributions are associated with the lighter quarks, leading to the branching fractions of  $\mathcal{B}(t \rightarrow cX) \simeq 10^{-15} - 10^{-12}$  [19], where X represents either a gluon (g), photon ( $\gamma$ ), Z, or a Higgs boson (h). Theoretical predictions for the top-quark FCNC effects are available with the next-to-leading order (NLO) precision [20,21], as well as the approximate next-to-next-to-next-to-leading order calculations for some of these processes [22,23].

The study of the flavour structure of the SM is one of the strongest probes of the beyond-the-SM (BSM) theories. A strong suppression of the top-quark FCNC transitions is a perfect condition to search for various possible deviations from the SM predictions. Several experimental studies of the properties of the FCNC decays of b hadrons have sparked a series of intriguing anomalies in the measured probabilities of the rare  $b \rightarrow sl^+\ell^-$  FCNC transitions, as well as in the measurements of the ratios  $\mathcal{B}(B^+ \rightarrow K^+\mu^+\mu^-)/\mathcal{B}(B^+ \rightarrow K^+e^+e^-)$  [24],  $\mathcal{B}(B^0 \rightarrow K^{*0}\mu^+\mu^-)/\mathcal{B}(B^0 \rightarrow K^{*0}e^+e^-)$  [25], as well as the branching fractions [26–28]. A common analysis of these results reveals a potential tension with respect to the SM [29–33]. The experimental searches for FCNC effects in the top-quark sector therefore represent an important channel to probe the anomalous interactions of the third-generation quarks.

## 2. Experimental Studies of the Top-Quark FCNC Processes

The top-quark FCNC effects can be probed directly in the production of a single top-quark, as well as in the top-quark decays, as shown in Figure 1. Studies of the top-quark FCNC decays are typically associated with similar sensitivities to the top-quark FCNC couplings with an up and a charm quark. Experimental sensitivities to these couplings mainly differ in terms of the performance of various reconstruction methods used for the identification of hadronic jets originating from quarks of a different flavour. At hadron colliders, the single top-quark FCNC production process is mostly sensitive to the top-quark FCNC coupling with an up quark (or an up antiquark) due to an enhanced sensitivity due to the proton distribution function of the colliding protons (or antiprotons). The importance of these two production channels depends on a specific type of the top-FCNC coupling that is probed in an experiment.

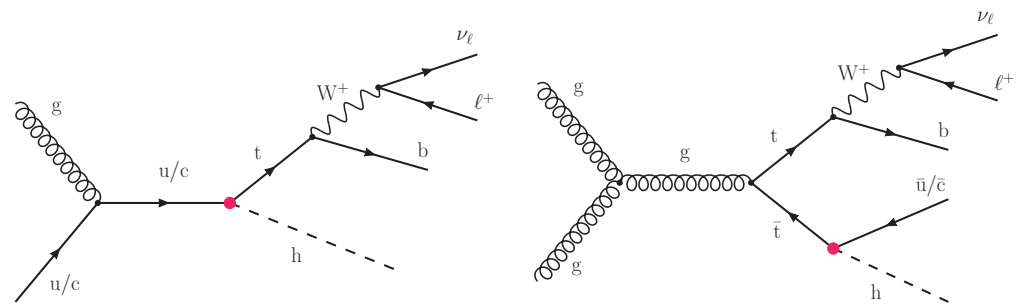


**Figure 1.** Representative leading-order Feynman diagrams for (left) single top quark and (right) top-quark pair production processes, involving top-Higgs FCNC couplings. The case of leptonic decays of the W boson is shown.

Before the LHC, the top-FCNC couplings were studied in electron–positron collisions at LEP2 [34–37], in deep inelastic scattering processes at HERA [38–42], and in proton–antiproton collisions at Tevatron [43–46]. The electron–positron colliders allow for a study of the top- $\gamma$  and top-Z couplings in the processes with the production of a single top quark,  $e^+e^- \rightarrow t\bar{c}(\bar{u})$ . The study of the deep inelastic scattering of electrons on protons has an enhanced sensitivity to the same type of couplings in the processes of  $ep \rightarrow et + X$ , as well as to the top-gluon FCNC couplings in the  $ep \rightarrow etq(g) + X$  processes. The obtained experimental constraints were recently improved by almost one order of magnitude after the analysis of the LHC proton–proton collision data [47–56].

The top-Higgs FCNC transitions receive the largest suppression in the SM with respect to the other top-quark FCNC processes because of the large mass of the Higgs boson. These transitions are among the rarest processes predicted in the SM in the quark sector, and therefore, the study of these processes is associated with a generally enhanced sensitivity to potential new physics effects. The discovery of the Higgs boson at the LHC paved a way to a comprehensive study of the top-Higgs FCNC processes at the ATLAS and CMS experiments, which resulted in the first experimental constraints on these anomalous couplings [57–65]. The direct searches for the top-Higgs FCNC effects are performed in top-quark decays, as well as in the associated production of single top quarks with a Higgs boson. Many of the performed studies were targeting the top-quark FCNC decays in  $t\bar{t}$  events. In recent studies of the 13 TeV data, the analysis of the single top-quark-associated production with a Higgs boson was also included [62–65].

### 2.1. $h \rightarrow \gamma\gamma$

Search channels that are relevant to the top-Higgs FCNC couplings are usually defined based on the Higgs boson decay channels. The Higgs boson decays to pairs of photons provide a clean experimental signature to look for the top-Higgs FCNC effects. In addition to the two photons, these final states consist of up to one isolated lepton with additional hadronic jets. The analysis strategy is primarily based on the reconstruction of the Higgs boson diphotonic invariant mass. The contributions from various background processes are fitted in the mass sidebands in the data, followed by its extrapolation to the signal region. In these fits, the background contributions that are associated with the SM Higgs boson production must be accounted for, representing one of the dominant resonant backgrounds in the search region. The uncertainty associated with the choice of the fit function, the statistical uncertainty in the data, as well as the background contributions from the SM processes involving the Higgs boson represent the main uncertainties in the study of these final states.

The searches for top-Higgs FCNC processes in the  $h \rightarrow \gamma\gamma$  channel were carried out by ATLAS [59] and CMS [63] in the single-lepton and hadronic final states, including a pair of photons (Figure 2). The integrated luminosity of the recorded 13 TeV data corresponds to 36 and 137  $\text{fb}^{-1}$ , respectively. The identification of isolated photon objects and the common vertex of the photon pair is the core part of the analysis. The photon

and the common vertex identification algorithms are based on the multivariate analysis (MVA) approaches. The obtained mass resolution allows the observation of a resonance structure in the diphoton invariant mass spectra in simulated signal events corresponding to the Higgs boson decay. The contributing nonresonant background processes include the diphoton production with jets, as well as the top-quark pair and the vector boson production processes with additional photons. The SM production of the Higgs boson represents the dominant resonant background. The nonresonant backgrounds are estimated directly from the data by performing a fit to the reconstructed diphoton invariant mass spectrum. The fitted function represents the sum of a double-sided Crystal Ball function that corresponds to the signal prediction, the resonant background from the SM Higgs production, and a parameterised function describing the nonresonant background obtained in a data control region. The main uncertainties include the b tagging and jet energy corrections, as well as the photon identification systematic uncertainties. The uncertainty in the limited number of events in the data also represents an important limiting factor in the final sensitivity in these searches. An additional contribution to the total systematic uncertainty is associated with theoretical uncertainties in the prediction of the resonant background processes with the SM Higgs boson production. The unbinned likelihood fit to the data using the described signal and background diphoton mass spectra is performed, and the constraints are set on the top-quark FCNC decay branching fractions. The observed (expected) limits obtained by ATLAS are  $\mathcal{B}(t \rightarrow hc) < 2.2 \times 10^{-3}$  ( $1.6 \times 10^{-3}$ ) and  $\mathcal{B}(t \rightarrow hu) < 2.4 \times 10^{-3}$  ( $1.7 \times 10^{-3}$ ). The observed (expected) constraints obtained in the CMS analysis are  $\mathcal{B}(t \rightarrow hc) < 7.3 \times 10^{-4}$  ( $5.1 \times 10^{-4}$ ) and  $\mathcal{B}(t \rightarrow hu) < 1.9 \times 10^{-4}$  ( $3.1 \times 10^{-4}$ ). An enhanced sensitivity obtained in the CMS analysis is explained by a larger data sample used in the study, as well as due to the inclusion of the top-Higgs FCNC process with the associated production of a single top quark and a Higgs boson. The latter has led to an improved sensitivity to  $\mathcal{B}(t \rightarrow hu)$ .

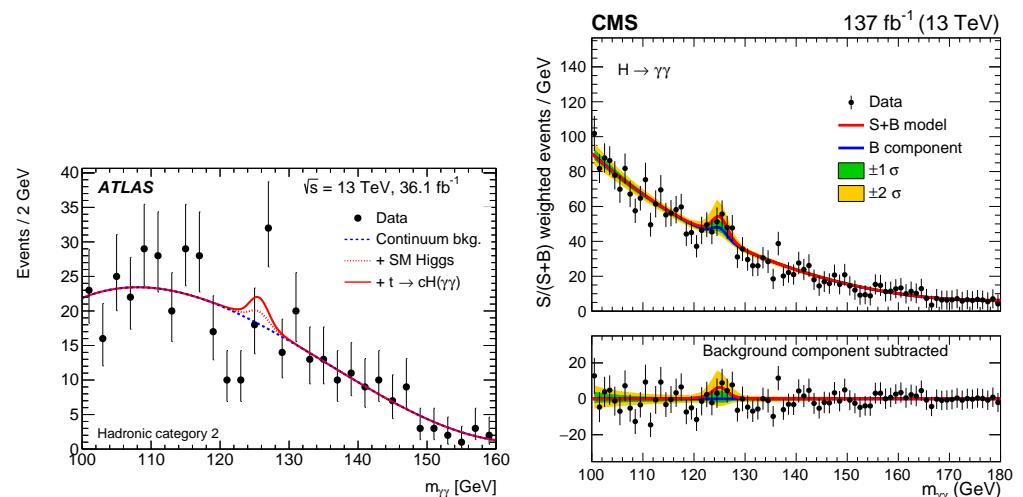


**Figure 2.** Distributions with the invariant diphoton mass showing the results of the fit to data in the top-Higgs FCNC study of the  $h \rightarrow \gamma\gamma$  channel at (left) ATLAS [59] and (right) CMS [63]. The ATLAS results are presented for hadronic final states, while the CMS results include a combination of all considered channels with events weighted by the associated significance of each event category.

### 2.2. $h \rightarrow WW/ZZ/\tau\tau$

Multilepton final states arise from the Higgs boson decays to a pair of W or Z bosons, as well as to  $\tau$  leptons. The event categories in these studies are associated with the final states with two same-sign or three selected leptons. The same-sign lepton channel has dominant background contributions originating from processes with nonprompt and misidentified leptons, while the three-lepton channel is mainly affected by the presence of diboson events as well as nonprompt leptons. These backgrounds are estimated from the data. The search channels involving one hadronic  $\tau$  lepton identified in the Higgs

boson decay receive the dominant background contributions from the processes with misidentified  $\tau$  lepton decays, as well as from events with the SM production of top quarks. In the case when the decays of both  $\tau$  leptons result in hadronic final states, a significant background contribution is also associated with the Z boson decays to the pairs of  $\tau$  leptons.

The searches for top-Higgs FCNC couplings in the multilepton channels were performed at ATLAS [58] and CMS [61] using  $36 \text{ fb}^{-1}$  of 13 TeV and  $20 \text{ fb}^{-1}$  of 8 TeV data, respectively. The events are split into the final states with two same-sign (2ISS) and three (3I) leptons. The dominant backgrounds are associated with the nonprompt and misidentified leptons, as well as with the leptons originating from photon conversions. The prompt-lepton backgrounds correspond to events with an associated production of top-quark pairs and a W, a Z, or a Higgs boson, with additional contributions arising from the processes with diboson production. The baseline selection criteria require the presence of two or three leptons and at least two jets, with one or two b-tagged jets. The prompt lepton identification plays an important role in these studies in suppressing the dominant nonprompt lepton backgrounds. The rejection of nonprompt leptons is usually achieved through an application of an MVA approach, which exploits a number of kinematic variables that provide a separation power between the two lepton categories, such as lepton isolation and properties of the reconstructed jet in proximity of the selected lepton. The statistical and systematic uncertainties associated with the prediction of the backgrounds with nonprompt leptons are among the dominant uncertainties in these searches. Two separate boosted decision tree (BDT) discriminants involving various reconstructed kinematic variables are trained in the 2ISS and 3I channels to further suppress various backgrounds. The BDT distributions that are presented in Figure 3 are used in a binned maximum likelihood fit to extract the constraints on the top-Higgs FCNC processes. The observed (expected) 95% CL limits on the top-quark FCNC branching fractions in the multilepton final states  $\mathcal{B}(t \rightarrow hc) < 1.6 \times 10^{-3}$  ( $1.5 \times 10^{-3}$ ) and  $\mathcal{B}(t \rightarrow hu) < 1.9 \times 10^{-3}$  ( $1.5 \times 10^{-3}$ ) are obtained. Multilepton searches provide an excellent sensitivity to the top-Higgs FCNC couplings; however, the existing results use only a partial data set, and further updates on these studies are anticipated in the future.

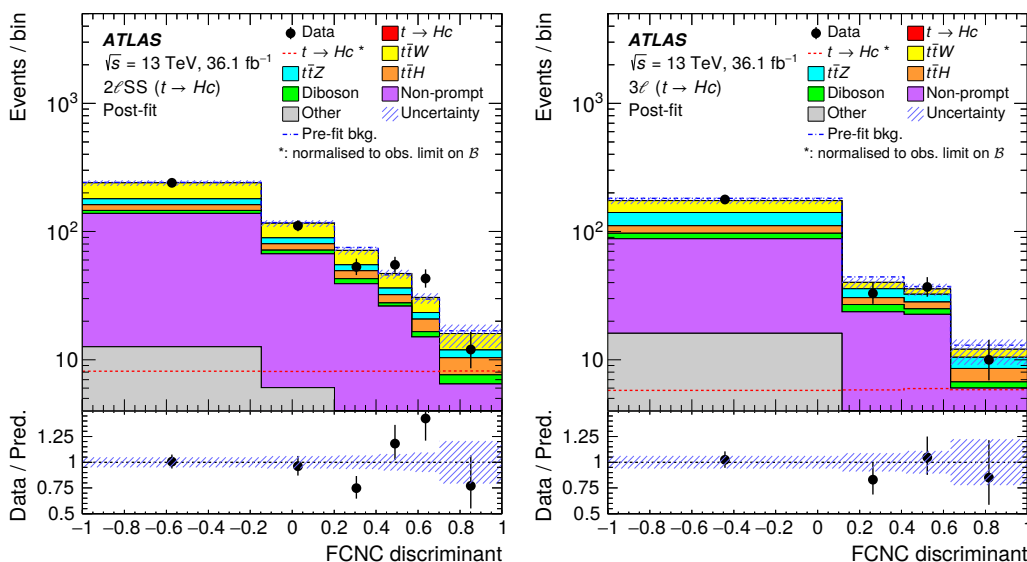


**Figure 3.** Distributions of the BDT discriminants using the top-Higgs FCNC signal selection in multilepton search channels in the same-sign dilepton (left) and trilepton (right) final states [58]. The presented BDT discriminant was optimised for the case of the  $t \rightarrow hc$  FCNC decays.

A dedicated study of the top-Higgs FCNC effects in the final states with one or two hadronically decaying  $\tau$  leptons was recently performed by ATLAS with  $139 \text{ fb}^{-1}$  of 13 TeV data [65]. The analysis strategy is similar to the one used in the previous analysis [57], with an increased number of kinematic regions sensitive to the signal pro-

duction, in order to account for the single-top production channel for the top-Higgs FCNC. The dominant background in this search is associated with the presence of nonprompt  $\tau$  leptons, estimated from the data. Other backgrounds are predicted by simulation. The obtained constraints on the branching fractions are  $\mathcal{B}(t \rightarrow hc) < 9.4 \times 10^{-4}$  ( $4.8 \times 10^{-4}$ ) and  $\mathcal{B}(t \rightarrow hu) < 6.9 \times 10^{-4}$  ( $3.5 \times 10^{-4}$ ).

### 2.3. $h \rightarrow b\bar{b}$

The Higgs boson decays to a pair of b quarks with the largest branching fraction of  $\simeq 58\%$  [66]. A considerable amount of background events is associated with the  $t\bar{t}$  production with additional hadronic jets. The analysis of this channel is systematically limited with the dominant contributions to the total uncertainty arising from the application of the heavy flavour jet identification techniques, as well as the modelling uncertainties relevant to the predictions of the top-quark production processes with additional jets. One of the important handles for suppressing background processes is the kinematic event reconstruction involving top quarks and additional jets. The assignment of the reconstructed final-state objects to the initial hard-process particles is performed using the MVA methods.

The top FCNC search in the  $h \rightarrow b\bar{b}$  channel is performed in the final states with one isolated lepton and additional jets. The total integrated luminosity used in the ATLAS analysis corresponds to  $36 \text{ fb}^{-1}$  of 13 TeV data [57]. The CMS results use  $101 \text{ fb}^{-1}$  of data [64], additionally combined with the previously published result from the analysis of  $36 \text{ fb}^{-1}$  data [62]. The ATLAS analysis focuses on the study of the event topology with at least four jets in the final state, mainly relevant to the top-quark FCNC decays. The corresponding CMS analysis additionally includes the signal top-quark production mode of the signal events, and therefore, the requirement on the minimum number of reconstructed jets is set to a lower value. At least three b-tagged jets are required to be present in the event. In both analyses, the selected events are classified based on the number of jets and b-tagged jets. The dominant background contributions correspond to the top-quark pair production in association with light-flavour jets in the event categories with two b-tagged jets, while the associated production of top-quark pairs with heavy-flavour jets ( $t\bar{t}b\bar{b}$  and  $t\bar{t}c\bar{c}$ ) represents the dominant background in the case of the higher number of b-tagged jets. The theoretical predictions for these processes are subject to relatively large uncertainties due to the renormalisation and the factorisation scale variations arising from the different energy scales of the top-quark mass and the jet transverse momentum involved in the generation process, as well as the inclusion of heavy quark masses in the calculations [67]. The experimental uncertainties in the measurement of the production cross sections of these processes reach  $\simeq 10\text{--}20\%$  [68–71]. The background processes are further suppressed by using the discriminants that exploit the kinematic information of the selected reconstructed objects, defining the probability of an event to correspond to the signal process hypothesis. As shown in Figure 4, in the ATLAS analysis, this is performed by constructing the likelihood (LH) discriminant, while the BDT approach is used in the case of the CMS search. The binned maximum likelihood fits are performed to the data based on the described discriminants to extract the limits on the FCNC contributions, resulting in the observed (expected) 95% CL constraints on the top-quark FCNC branching fractions of  $\mathcal{B}(t \rightarrow hc) < 4.2 \times 10^{-3}$  ( $4.0 \times 10^{-3}$ ) and  $\mathcal{B}(t \rightarrow hu) < 5.2 \times 10^{-3}$  ( $4.9 \times 10^{-3}$ ). The resultant constraints in the CMS analysis are  $\mathcal{B}(t \rightarrow hc) < 9.4 \times 10^{-4}$  ( $8.6 \times 10^{-4}$ ) and  $\mathcal{B}(t \rightarrow hu) < 7.9 \times 10^{-4}$  ( $1.1 \times 10^{-3}$ ). The differences in the sensitivities in the published results by the two experiments are mainly due to the different size of the analysed data sample, as well as to the inclusion of the single top-quark production mode for the top-Higgs FCNC process in the case of the CMS analysis. A combination of the results obtained from the analyses of different Higgs boson decay channels,  $h \rightarrow \gamma\gamma$ ,  $h \rightarrow WW/ZZ$ ,  $h \rightarrow \tau\tau$ , and  $h \rightarrow b\bar{b}$ , was performed at ATLAS using  $36 \text{ fb}^{-1}$  of data, corresponding to the limits of  $\mathcal{B}(t \rightarrow hc) < 1.1 \times 10^{-3}$  ( $8.3 \times 10^{-4}$ ) and  $\mathcal{B}(t \rightarrow hu) < 1.1 \times 10^{-3}$  ( $8.3 \times 10^{-4}$ ) [57]. The ATLAS constraints on the top-Higgs FCNC interactions are competitive to the ones

obtained in the analysis of the  $h \rightarrow \gamma\gamma$  channel at CMS [63], which already uses all the available recorded data at 13 TeV.

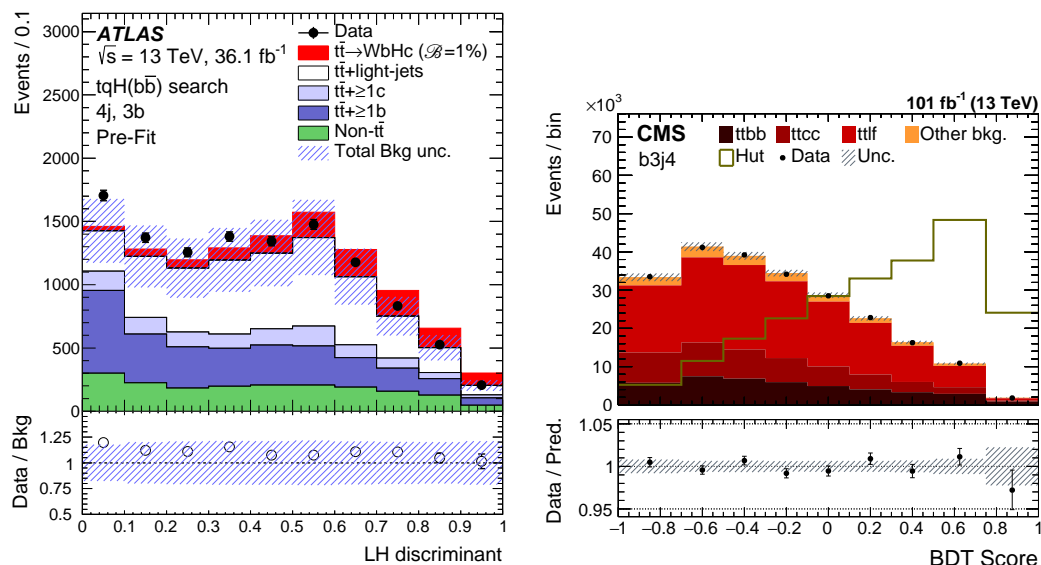


**Figure 4.** Distributions of the discriminants used in the analyses of the  $h \rightarrow b\bar{b}$  channel at (left) ATLAS [57] and (right) CMS [64]. Selected events correspond to the final states with four reconstructed jets, three of which are identified as associated with heavy-flavour hadron decays. The pre-fit and post-fit results are shown for ATLAS and CMS, respectively.

### 2.4. Indirect Searches

The top-Higgs FCNC interactions can be indirectly constrained from the studies of the SM processes that can potentially include FCNC loop-level contributions involving top quarks. The relevant processes include the hadron electric dipole moments [72,73],  $Z \rightarrow c\bar{c}$  decays [74], and  $D^0 - \bar{D}^0$  mixing [75]. The indirect limits are competitive with the current direct constraints obtained at the LHC [76].

## 3. Global Approach to the FCNC Searches

A broad range of experimental searches for new physics phenomena have been using the  $\kappa$ -framework to parameterise the potential deviations from the SM predictions [77]. This framework defines a set of scaling factors for production cross sections and decay widths as a function of the new physics model parameters. While the  $\kappa$ -framework has proved to be very successful in theoretical interpretations of a large number of experimental results, it does not represent an ultimate approach to providing a complete systematic description of various new physics effects.

Given the absence of any strong evidence of new physics, the natural assumption is that new particles are much heavier than the SM particles, and its direct production at present is not achievable within the LHC energy range. The potentially induced new physics effects at the electroweak scale can be parameterised with a general effective field theory (EFT) approach that includes additional high-energy dimensional operators in the extended Lagrangian of the SM (SMEFT). The rich phenomenology of the SMEFT includes 59 independent operators, assuming baryon number conservation [78,79]. A full categorisation of EFT operators relevant to the top-quark sector and its interplay with other SM processes is summarised in refs. [80–82]. Several of these operators are relevant to the FCNC processes with top quarks. The Wilson coefficients (WCs) of the respective EFT operators can be constrained from the measured production cross sections, as well as from the study of the shapes of various kinematic variables. An EFT analysis of experimental observables represents a general approach to study potential deviations from the SM predictions that can be used to set constraints on various BSM models. The top-quark

FCNC EFT couplings comprise several dimension-six operators, which are discussed in refs. [81–85]. The FCNC EFT contributions can also interfere at higher orders [83,84,86].

The potential FCNC EFT effects with top quarks were probed in the experimental studies of top-gluon and top-photon FCNC processes at the LHC [56,87]. Additionally, several of the obtained experimental constraints on the FCNC top-quark decay branching fractions and strength  $\kappa$ -modifiers, which were described in Section 2, can be directly translated into the corresponding limits on the relevant WCs. The first direct measurement of the constraints on the EFT WCs relevant to the top-Higgs FCNC interactions was recently performed in ref. [65]. The re-interpretations of various experimental results that are sensitive to the top-Higgs EFT operators are also available [80,84].

#### 4. New Scalar Bosons

Several extensions of the SM can induce sizable FCNC effects that can be experimentally probed at the LHC. There are two possible ways to introduce the top-quark FCNC in a BSM model. The first possibility is to increase the number of fermions, modifying the CKM matrix structure, escaping the GIM suppression. This approach is usually referred to as the minimal flavour violation (MFV). The second option is to involve new heavy particles in the loops of the higher-order diagrams, increasing the probability of FCNC transitions. The study of top-Higgs FCNC effects appears to be rather promising in various simple extensions of the SM, where the additional neutral scalar particles can potentially mix with the SM Higgs boson.

A dedicated estimate of the BSM-enhanced branching fractions of  $t \rightarrow u(c)h$  decays shows the maximal values reaching  $10^{-3} - 10^{-4}$  in some BSM models [19,88]. Such high event rates are being probed at the LHC using recorded data with the typical constraints set at the level of  $\simeq 10^{-3}$ . However, the maximal branching fractions are not necessarily associated with the most favourable parameter space of a BSM model and can potentially involve additional model tuning.

The SM Higgs boson can have its additional partners in various BSM scenarios. The two-Higgs doublet model (2HDM) is one of the simplest extensions of the SM that introduces two Higgs doublets with five scalar particles:  $h^0$ , CP-odd  $A^0$ , CP-even  $H^0$  ( $m_H > m_h$ ), and  $H^\pm$ , where  $h^0$  is the lightest CP-even SM-like Higgs boson [89–91]. The 2HDM contains seven parameters, with only two of them relevant at the leading order (LO), usually defined as  $\cos(\beta - \alpha)$  and  $\tan(\beta)$ . The former parameter is related to the couplings of a scalar particle to vector bosons, while the latter represents the ratio of the vacuum expectation values of the heavy and the SM Higgs bosons.

There are four (I, II, III, and IV) types of 2HDM. The 2HDM-I and 2HDM-II do not include FCNC processes at the tree level due to the requirement of flavour conservation via the presence of a  $Z_2$  symmetry. In these two types of 2HDM, all the fermions couple to the same Higgs boson. In the 2HDM-III without an imposed discrete symmetry, the fermions can couple to both Higgs doublets, and the tree-level FCNC transitions involving the top-charm FCNC couplings with the Higgs boson can be significantly enhanced [92]. A combined fit of various results from the direct and indirect experimental searches favours the alignment limit  $\cos(\beta - \alpha) \rightarrow 0$  with  $\cos(\beta - \alpha) < 0.1 - 0.4$ , with some additional dependence on  $\tan(\beta)$ , the mass of the scalar boson, as well as the type of the model [93–105]. The alignment scenario corresponds to the case, when  $h^0$  and the SM Higgs boson share the same couplings.

In the aligned two-Higgs doublet model (A2HDM), it is assumed that both Yukawa matrices are aligned in the flavour space to avoid the FCNC at the tree level [96]. The enhanced one-loop-induced  $t \rightarrow ch$  decays can occur in such models [97]. Special extensions of the 2HDM models can incorporate the FCNC at the tree level, such as the top-quark 2HDM (T2HDM) [98]. In this model, it is assumed that the top quark is the only elementary fermion that couples to the non-SM Higgs doublet to generate its large mass in a natural way, therefore allowing the top-Higgs FCNC due to a small  $\cos(\beta - \alpha)$  admixture of the exotic neutral Higgs boson. The study of the  $t \rightarrow ch$  decays represents a promising channel

to probe the T2HDM and 2HDM-III at the LHC [99–102]. There are also the so-called BGL modifications of the 2HDM, where the tree-level top-Higgs FCNC transitions can be associated with either up- or down-type quarks, preserving the structure of the CKM matrix [103–105].

Additional Higgs doublets can naturally appear in the context of supersymmetric (SUSY) theories. The minimal supersymmetric standard model (MSSM) is the simplest extension of the SM representing the 2HDM-II with additional supersymmetric particle content [106–108]. At the tree level, this model contains two non-SM parameters: the mass of the CP-odd Higgs boson,  $m_A$ , and  $\tan(\beta)$ . An effective MSSM with the lightest CP-even SM Higgs boson is referred to as the hMSSM, where the properties of the SM Higgs boson define the remaining masses and couplings of the MSSM [91,109,110]. This approximation of MSSM is only completely valid at the moderate values of  $\tan(\beta)$ . The recent LHC experimental searches generally disfavour small values of  $m_A$  below  $\simeq 600$  GeV within the hMSSM [93–105]. The predicted top-Higgs FCNC rates in a general MSSM can reach  $10^{-7}$  [111], while in the case of the R-parity violation (RPV) in a general SUSY model, these transitions can be enhanced to  $10^{-5}$  [112].

An extended MSSM with baryon (B) and lepton (L) numbers as local symmetries, broken near the electroweak scale, is known as BLMSSM [113–116]. This model can incorporate an enhancement of  $t \rightarrow ch$  rates at one loop [117]. The next-to-minimal supersymmetric standard model (NMSSM) represents an extension of the MSSM that naturally generates the mass parameter  $\mu$  in the Higgs superpotential at the electroweak scale and resolves the so-called  $\mu$ -problem [118,119]. The new neutral scalars considered in the MSSM theories can potentially mix with the SM Higgs boson and therefore generate top-Higgs FCNC at the tree level.

The addition of the exotic vector-like quark to the CKM matrix provides a way to escape the GIM mechanism. The top-Higgs FCNC transitions can be enhanced to  $10^{-5}$  in the quark singlet (QS) [120] and alternative left-right models (ALRM) [121]. Similar enhancements can be achieved in the Littlest Higgs Model with T-parity (LHT) induced by interactions with the new T-odd gauge bosons and fermions [122]. The presence of the Kaluza–Klein fermion states in the Randall–Sundrum (RS) models with warped extra dimensions can produce sizable FCNC effects of the same order [123–125].

The new light neutral scalar singlets (S) are present in various supersymmetric extensions of the SM, including the NMSSM and the composite Higgs models (CHM) [126–130], with  $t \rightarrow cS$  tree-level FCNC decays [131]. In such extensions, these scalars are considered as Nambu–Goldstone bosons (pNGBs) with the Higgs boson, representing a bound state of new strongly interacting dynamics. The large mass of the top quark can be generated through the mixing of elementary fermions with a composite operator of a high scaling dimension [132]. In CHM, the SM elementary particles can be seen as composite states that mix with its heavy partners. This model provides a promising explanation of the mass hierarchy of the SM by introducing a new physics scale and the idea of compositeness of the SM particles. The  $t \rightarrow cS$  decays, with  $m_S < m_t - m_c$ , are expected to strongly dominate over the  $t \rightarrow ch$  transitions in the CHM, providing a new window to constrain the new physics models via the top-quark FCNC searches with neutral light scalars. These processes are not yet studied experimentally. The predicted rates of the  $t \rightarrow cS$  decays can be probed down to  $10^{-5}$  with the existing LHC data [129,130].

In addition to the top-quark FCNC decays with a Higgs boson, one can also search for FCNC decays of the heavy neutral scalars (H) predicted in many BSM models. In a general 2HDM model, as well as in its extensions, such as the T2HDM, the probability of the  $H \rightarrow t\bar{c}$  decay is proportional to  $\sin(\beta - \alpha)$ , while the probabilities of the  $t \rightarrow ch$  decays are proportional to  $\cos(\beta - \alpha)$  [133–137]. This represents an important complementarity of the top FCNC searches in the top-quark and heavy neutral scalar decays. At high energies, one of the dominant decays of the heavy scalars is the production of two top quarks, if the mass of the scalar particle exceeds the doubled mass of the top quark. However, in the heavy scalar mass range of 175 and 350 GeV, the  $H \rightarrow t\bar{c}$  decays are

associated with the largest branching fraction in the model parameter space, favoured by the current experimental constraints [138]. A study of the  $H \rightarrow t\bar{c}$  decays is a promising way to search for heavy neutral scalar particles at the LHC [133–137]. The dominant production mode for heavy scalars is expected to be the gluon–gluon fusion process; however, in the context of the “flavorful” 2HDM (F2HDM), that removes the 2HDM-intrinsic  $Z_2$  discrete symmetry and additionally modifies the structure of the Yukawa matrices [139–141], the dominant channel is the single top-associated production with a heavy neutral scalar ( $pp \rightarrow tH \rightarrow t\bar{c}$ ), resulting in the presence of two same-sign top quarks in the final state [142]. Similar final states are relevant to the top-quark FCNC searches within the T2HDM [133–137]. The searches for the heavy scalar FCNC decays with top quarks are also proposed within the Froggatt–Nelsen singlet model (FNSM), mostly relevant for the HL-LHC data analysis [143].

## 5. Future Perspectives

The LHC has accumulated about  $25 \text{ fb}^{-1}$  of proton–proton collision data at 7 and 8 TeV, as well as nearly  $140 \text{ fb}^{-1}$  of data at 13 TeV. The latest studies from the LHC on the top-quark FCNC processes therefore focus on the analysis of the 13 TeV data. The next round of the data taking at the LHC is planned for 2022, where it is expected that the total accumulated statistics will be doubled, reaching  $300 \text{ fb}^{-1}$  by the end of the LHC project. The future experiments at the High-Luminosity LHC (HL-LHC) are planned to bring almost an order of magnitude larger data set of  $3 \text{ ab}^{-1}$  due to a significant increase in the instantaneous luminosity of the colliding proton beams up to  $10^{35} \text{ cm}^{-2} \text{ s}^{-1}$ , representing a 5 to 7 times higher luminosity with respect to its nominal value. The projected sensitivities of the top-quark FCNC searches, following the preliminary estimates of the expected performances of the upgraded ATLAS and CMS detectors at the HL-LHC, indicate a significant improvement in the constraints on the branching fractions of the top-quark FCNC decays after the analysis of the full LHC statistics, reaching an order of magnitude [144].

There are several major international projects under consideration in the high-energy physics domain, defining an evolving strategy for this field for many years to come. The Large Hadron electron Collider (LHeC) is proposed as an extension of the LHC project, re-using the existing proton accelerator complex and combining it with a new electron accelerator for the production of 60 GeV electron beams for the study of the deep inelastic scattering at high energies [145–148]. The planned experiments at the LHeC are mostly sensitive to the top- $\gamma/Z$  FCNC couplings, and the projected limits are expected to be comparable to the corresponding sensitivities at the HL-LHC [149–151]. The study of the top-Higgs FCNC interactions appears to be less promising at the LHeC, the expected sensitivity of which has been already surpassed by the latest LHC results [152].

The electron–proton collisions are considered as part of the Future Circular Collider (FCC) project, involving several experiments targeting different types of high-energy collisions. The FCC-eh machine will collide a 60 GeV electron with 50 TeV proton beams, produced by the FCC accelerator [153,154]. Due to the increased energy of the proton beams, relatively similar sensitivities for the top-Higgs FCNC couplings are expected to the ones of the HL-LHC. Most of the improvements are anticipated for the top- $\gamma/Z$  FCNC couplings [144,155]. The planned experiments at the high-precision electron–positron collider (FCC-ee) will also be very sensitive to the top- $\gamma/Z$  FCNC couplings [156]. The dominant sensitivity to the top-Higgs FCNC processes at the FCC-ee is mainly associated with the top-quark decay channels. The FCC-hh machine with proton–proton collisions at  $\sqrt{s} = 100 \text{ TeV}$  will allow increased sensitivity to all relevant top-quark FCNC couplings, probing the  $t \rightarrow ch$  decay branching fractions down to  $\simeq 10^{-5}$  [157–161]. The High-Energy LHC (HE-LHC) project will adopt the FCC-hh technology to use proton–proton collisions at  $\sqrt{s} = 27 \text{ TeV}$ . The HE-LHC is viewed as capable to improve the HL-LHC limits on the top-quark FCNC couplings by an order of magnitude [162,163]. The linear electron–positron colliders, such as the ILC and CLIC, are also associated with good prospects for the top-quark FCNC studies [164–168]. However, the projected ILC/CLIC sensitivities

for the top-Higgs FCNC interactions are not expected to reach the sensitivity level of the corresponding studies at the HL-LHC.

A summary of the described experimental results and future projections is presented in Figure 5. The analysis of the  $\simeq 140 \text{ fb}^{-1}$  of the LHC 13 TeV data allows reaching the 95% confidence level limits of the order of  $10^{-4}$  and  $10^{-3}$  for the  $t \rightarrow uh$  and  $t \rightarrow ch$  decay branching fractions, respectively. These experimental limits are obtained from the analysis of the the Higgs boson decays to photon pairs, and therefore, the presented results are expected to be further improved when combined with the results obtained in the analysis of other Higgs boson’s decay modes. The illustrated sensitivities for future colliders are also obtained in the analyses of specific channels. The comparison with the ultimate sensitivities is expected to be more complete, once the LHC and the future projection results become available for all the relevant decay channels of the Higgs boson. Based on the considered projections, the best expected sensitivity of  $\simeq 10^{-5}$  is associated with the experiments at the FCC-hh.

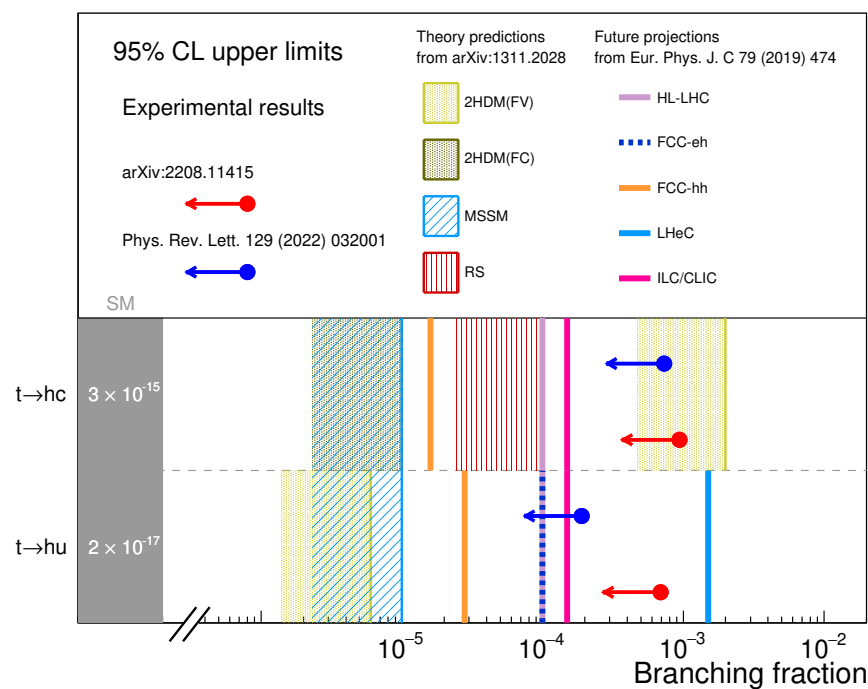


**Figure 5.** Summary of the best experimental constraints to date on the top-Higgs FCNC processes at the LHC [63,65], including sensitivity projections for future colliders. The results are also compared to various BSM predictions that correspond to the maximal expected branching fractions in a given model. Adapted from ref. [144].

The described sensitivities of the future experiments mainly correspond to the studies of the top-Higgs FCNC couplings, with only a few projections available for some of the top-quark flavour-changing neutral scalar processes. While the searches for new scalars via the top-quark FCNC appear to be highly relevant for the HL-LHC, as well as its successors, these processes are not yet explored to the full extent with the existing LHC data.

### 6. Summary

The sensitivity of the LHC experiments has reached the level of being able to rule out several BSM models assuming the maximal branching fractions of the top-quark FCNC decays. The study of the top-quark FCNC processes involving the neutral scalar bosons is an excellent probe of the new physics effects in a number of BSM scenarios, including additional Higgs doublets and scalar singlets through partial compositeness. In some models, the production of new scalars can be significantly enhanced by the flavour-changing neutral scalar couplings, and therefore, these studies represent a very promising

direction to look for additional heavy and light partners of the discovered Higgs boson. Beyond the LHC, the upcoming experiments at the HL-LHC and FCC are expected to come with even better sensitivities to probe the top-quark anomalous couplings with the new scalars. The analysis of the LHC and the future collider data will remain the only way to directly probe the top-quark flavour-changing neutral scalar interactions in the next decades.

**Funding:** This research received no external funding.

**Informed Consent Statement:** Not applicable.

**Data Availability Statement:** Not applicable.

**Acknowledgments:** NC is supported by the FCT—Fundação para a Ciências e a Tecnologia, Portugal, under project CERN/FIS-PAR/0032/2021.

**Conflicts of Interest:** The authors declare no conflict of interest.

## References

1. Kobayashi, M.; Maskawa, T. CP violation in the renormalizable theory of weak interaction. *Prog. Theor. Phys.* **1973**, *49*, 652. [[CrossRef](#)]
2. Glashow, S.L.; Iliopoulos, J.; Maiani, L. Weak interactions with lepton-hadron symmetry. *Phys. Rev. D* **1970**, *2*, 1285. [[CrossRef](#)]
3. Cabibbo, N. Unitary symmetry and leptonic decays. *Phys. Rev. Lett.* **1963**, *10*, 531. [[CrossRef](#)]
4. Maiani, L. The GIM Mechanism: Origin, predictions and recent uses. *arXiv* **2013**, arXiv:1303.6154.
5. Augustin, J.-E. et al. [SLAC Collaboration]. Discovery of a narrow resonance in  $e^+e^-$  annihilation. *Phys. Rev. Lett.* **1974**, *33*, 1406. [[CrossRef](#)]
6. Aubert, J.J. et al. [E598 Collaboration]. Experimental observation of a heavy particle. *J. Phys. Rev. Lett.* **1974**, *33*, 1404. [[CrossRef](#)]
7. Herb, S.W. et al. [E288 Collaboration]. Observation of a dimuon resonance at 9.5 GeV in 400 GeV proton-nucleus collisions. *Phys. Rev. Lett.* **1977**, *39*, 252. [[CrossRef](#)]
8. Abe, F. et al. [CDF Collaboration]. Observation of top quark production in  $\bar{p}p$  collisions. *Phys. Rev. Lett.* **1995**, *74*, 2626. [[CrossRef](#)]
9. Abachi, S. et al. [D0 Collaboration]. Search for high mass top quark production in  $p\bar{p}$  collisions at  $\sqrt{s} = 1.8$  TeV. *Phys. Rev. Lett.* **1995**, *74*, 2422. [[CrossRef](#)]
10. de Gouvêa, A.; Vogel, P. Lepton flavor and number conservation, and physics beyond the standard model. *Prog. Part. Nucl. Phys.* **2013**, *71*, 75. [[CrossRef](#)]
11. Celi, F.; Nicolo, D. Lepton flavour violation experiments. *Adv. High Energy Phys.* **2014**, *2014*, 282915. [[CrossRef](#)]
12. Calibbi, L.; Signorelli, G. Charged lepton flavour violation: An experimental and theoretical introduction. *Riv. Nuovo C.* **2018**, *41*, 71. [[CrossRef](#)]
13. Aubert, B. et al. [BaBar Collaboration]. Measurements of the  $B \rightarrow X_s \gamma$  branching fraction and photon spectrum from a sum of exclusive final states. *Phys. Rev. D* **2005**, *72*, 052004. [[CrossRef](#)]
14. Nishimura, K. et al. [Belle Collaboration]. First measurement of inclusive  $B \rightarrow X_s \eta$  decays. *Phys. Rev. Lett.* **2010**, *105*, 191803. [[CrossRef](#)] [[PubMed](#)]
15. Mohapatra, D. et al. [Belle Collaboration]. Observation of  $b \rightarrow d \gamma$  and determination of  $V_{td}/V_{ts}$ . *Phys. Rev. Lett.* **2006**, *96*, 221601. [[CrossRef](#)]
16. Lin, S.-W. et al. [Belle Collaboration]. Observation of  $B$  decays to two kaons. *Phys. Rev. Lett.* **2007**, *98*, 181804. [[CrossRef](#)]
17. Lees, J.P. et al. [BaBar Collaboration]. Searches for rare or forbidden semileptonic charm decays. *Phys. Rev. D* **2011**, *84*, 072006. [[CrossRef](#)]
18. Batley, J.R. et al. [NA48/2 Collaboration]. Precise measurement of the  $K^\pm \rightarrow \pi^\pm e^+ e^-$  decay. *Phys. Lett. B* **2009**, *677*, 246. [[CrossRef](#)]
19. Aguilar-Saavedra, J.A. Top flavour-changing neutral interactions: Theoretical expectations and experimental detection. *Acta Phys. Polon. B* **2004**, *35*, 2695.
20. Zhang, J.J.; Li, C.S.; Gao, J.; Zhang, H.; Li, Z.; Yuan, C.-P.; Yuan, T.-C. Next-to-leading-order QCD corrections to the top-quark decay via model-independent flavor-changing neutral-current couplings. *Phys. Rev. Lett.* **2009**, *102*, 072001. [[CrossRef](#)]
21. Zhang, C.; Maltoni, F. Top-quark decay into Higgs boson and a light quark at next-to-leading order in QCD. *Phys. Rev. D* **2013**, *88*, 054005. [[CrossRef](#)]
22. Forslund, M.; Kidonakis, N. Soft-gluon corrections for single top quark production in association with electroweak bosons. *arXiv* **2019**, arXiv:1909.02619.
23. Guzzi, M.; Kidonakis, N.  $tZ'$  production at hadron colliders. *Eur. Phys. J. C* **2020**, *80*, 467. [[CrossRef](#)]
24. Aaij, R. et al. [LHCb Collaboration]. Search for lepton-universality violation in  $B^+ \rightarrow K^+ \ell^+ \ell^-$  decays. *Phys. Rev. Lett.* **2019**, *122*, 191801. [[CrossRef](#)]

25. Aaij, R. et al. [LHCb Collaboration]. Test of lepton universality with  $B^0 \rightarrow K^{*0} \ell^+ \ell^-$  decays. *JHEP* **2017**, *8*, 55. [[CrossRef](#)]
26. Aaij, R. et al. [LHCb Collaboration]. Differential branching fractions and isospin asymmetries of  $B \rightarrow K^{(*)} \ell^+ \ell^-$  decays. *JHEP* **2014**, *6*, 133. [[CrossRef](#)]
27. Aaij, R. et al. [LHCb Collaboration]. Measurements of the S-wave fraction in  $B^0 \rightarrow K^+ \pi \mu^+ \mu^-$  decays and the  $B^0 \rightarrow K^*(892)^0 \mu^+ \mu^-$  differential branching fraction. *JHEP* **2016**, *11*, 47. Erratum: *JHEP* **2017**, *4*, 142. [[CrossRef](#)]
28. Aaij, R. et al. [LHCb Collaboration]. Angular analysis and differential branching fraction of the decay  $B_s^0 \rightarrow \phi \mu^+ \mu^-$ . *JHEP* **2015**, *9*, 179. [[CrossRef](#)]
29. D'Amico, G.; Nardecchia, M.; Panci, P.; Sannino, F.; Strumia, A.; Torre, R.; Urbano, A. Flavour anomalies after the  $R_{K^*}$  measurement. *JHEP* **2017**, *9*, 10. [[CrossRef](#)]
30. Capdevila, B.; Crivellin, A.; Descotes-Genon, S.; Matias, J.; Virto, J. Patterns of new physics in  $b \rightarrow s \ell^+ \ell^-$  transitions in the light of recent data. *JHEP* **2018**, *1*, 93. [[CrossRef](#)]
31. Arbey, A.; Hurth, T.; Mahmoudi, F.; Neshatpour, S. Hadronic and new physics contributions to  $b \rightarrow s$  transitions. *Phys. Rev. D* **2018**, *98*, 095027. [[CrossRef](#)]
32. Kim, T. J.; Ko, P.; Li, J.; Park, J.; Wu, P. Correlation between  $R_{D^{(*)}}$  and top quark FCNC decays in leptoquark models. *JHEP* **2019**, *7*, 25. [[CrossRef](#)]
33. Bansal, S.; Capdevilla, R.M.; Kolda, C. On the Minimal Flavor Violating Leptoquark explanation of the  $R_{D^{(*)}}$  anomaly. *Phys. Rev. D* **2019**, *99*, 035047. [[CrossRef](#)]
34. Achard, P. et al. [L3 Collaboration]. Search for single top production at LEP. *Phys. Lett. B* **2002**, *549*, 290. [[CrossRef](#)]
35. Abbiendi, G. et al. [OPAL Collaboration]. Search for single top quark production at LEP2. *Phys. Lett. B* **2001**, *521*, 181. [[CrossRef](#)]
36. Barate, R. et al. [ALEPH Collaboration]. Search for single top production in  $e^+ e^-$  collisions at  $\sqrt{s} = 189$  GeV - 202 GeV. *Phys. Lett. B* **2000**, *494*, 33. [[CrossRef](#)]
37. Abdallah, J. et al. [DELPHI Collaboration]. Search for single top production via FCNC at LEP at  $\sqrt{s} = 189$  GeV - 208 GeV. *Phys. Lett. B* **2005**, *590*, 21. [[CrossRef](#)]
38. Aktas, A. et al. [H1 Collaboration]. Search for single top quark production in  $ep$  collisions at HERA. *Eur. Phys. J. C* **2004**, *33*, 9. [[CrossRef](#)]
39. Chekanov, S. et al. [ZEUS Collaboration]. Search for single-top production in  $ep$  collisions at HERA. *Phys. Lett. B* **2003**, *559*, 153–170. [[CrossRef](#)]
40. Abramowicz, H. et al. [ZEUS Collaboration]. Search for single-top production in  $ep$  collisions at HERA. *Phys. Lett. B* **2012**, *708*, 27. [[CrossRef](#)]
41. Aaron, F.D. et al. [H1 Collaboration]. Search for single top quark production at HERA. *Phys. Lett. B* **2009**, *678*, 450. [[CrossRef](#)]
42. Heister, A. et al. [ALEPH Collaboration]. Search for single top production in  $e^+ e^-$  collisions at  $\sqrt{s}$  up to 209 GeV. *Phys. Lett. B* **2002**, *543*, 173. [[CrossRef](#)]
43. Abazov, V. et al. [D0 Collaboration]. Search for flavor changing neutral currents via quark-gluon couplings in single top quark production using  $2.3 \text{ fb}^{-1}$  of  $p\bar{p}$  collisions. *Phys. Lett. B* **2010**, *693*, 81. [[CrossRef](#)]
44. Abazov, V. et al. [D0 Collaboration]. Search for production of single top quarks via  $t c g$  and  $t u g$  flavor-changing-neutral-current couplings. *Phys. Rev. Lett.* **2007**, *99*, 191802. [[CrossRef](#)]
45. Aaltonen, T. et al. [CDF Collaboration]. Search for the flavor-changing neutral-current decay  $t \rightarrow Z q$  in  $p\bar{p}$  collisions at  $\sqrt{s} = 1.96$  TeV. *Phys. Rev. Lett.* **2008**, *101*, 192002. [[CrossRef](#)]
46. Aaltonen, T. et al. [CDF Collaboration]. Search for top-quark production via flavor-changing neutral currents in W+1 jet events at CDF. *Phys. Rev. Lett.* **2009**, *102*, 151801. [[CrossRef](#)]
47. Sirunyan, A. et al. [CMS Collaboration]. Search for associated production of a Z boson with a single top quark and for tZ flavour-changing interactions in  $pp$  collisions at  $\sqrt{s} = 8$  TeV. *JHEP* **2017**, *7*, 003. [[CrossRef](#)]
48. Khachatryan, V. et al. [CMS Collaboration]. Search for anomalous Wtb couplings and flavour-changing neutral currents in t-channel single top quark production in  $pp$  collisions at  $\sqrt{s} = 7$  and 8 TeV. *JHEP* **2017**, *2*, 28. [[CrossRef](#)]
49. Khachatryan, V. et al. [CMS Collaboration]. Search for anomalous single top quark production in association with a photon in  $pp$  collisions at  $\sqrt{s} = 8$  TeV. *JHEP* **2016**, *4*, 35. [[CrossRef](#)]
50. Chatrchyan, S. et al. [CMS Collaboration]. Search for flavor changing neutral currents in top quark decays in  $pp$  collisions at  $\sqrt{s} = 7$  TeV. *Phys. Lett. B* **2013**, *718*, 1252. [[CrossRef](#)]
51. Chatrchyan, S. et al. [CMS Collaboration]. Search for flavor-changing neutral currents in top-quark decays  $t \rightarrow Z q$  in  $pp$  collisions at  $\sqrt{s} = 8$  TeV. *Phys. Rev. Lett.* **2014**, *112*, 171802. [[CrossRef](#)] [[PubMed](#)]
52. Aaboud, M. et al. [ATLAS Collaboration]. Search for flavour-changing neutral current top-quark decays  $t \rightarrow q Z$  in proton-proton collisions at  $\sqrt{s} = 13$  TeV with the ATLAS detector. *JHEP* **2018**, *7*, 176. [[CrossRef](#)]
53. Aad, G. et al. [ATLAS Collaboration]. Search for single top-quark production via flavour changing neutral currents at 8 TeV with the ATLAS detector. *Eur. Phys. J. C* **2016**, *76*, 55. [[CrossRef](#)] [[PubMed](#)]
54. Aad, G. et al. [ATLAS Collaboration]. Search for flavour-changing neutral current top-quark decays to  $q Z$  in pp collision data collected with the ATLAS detector at  $\sqrt{s} = 8$  TeV. *Eur. Phys. J. C* **2016**, *76*, 12. [[CrossRef](#)] [[PubMed](#)]
55. Aad, G. et al. [ATLAS Collaboration]. A search for flavour changing neutral currents in top-quark decays in  $pp$  collision data collected with the ATLAS detector at  $\sqrt{s} = 7$  TeV. *Eur. Phys. J. C* **2012**, *9*, 139. [[CrossRef](#)]

56. Aad, G. et al. [ATLAS Collaboration]. Search for flavour-changing neutral currents in processes with one top quark and a photon using  $81 \text{ fb}^{-1}$  of  $pp$  collisions at  $\sqrt{s} = 13 \text{ TeV}$  with the ATLAS experiment. *Phys. Lett. B* **2019**, *800*, 135082. [[CrossRef](#)]
57. Aaboud, M. et al. [ATLAS Collaboration]. Search for top-quark decays  $t \rightarrow Hq$  with  $36 \text{ fb}^{-1}$  of  $pp$  collision data at  $\sqrt{s} = 13 \text{ TeV}$  with the ATLAS detector. *JHEP* **2019**, *5*, 123. [[CrossRef](#)]
58. Aaboud, M. et al. [ATLAS Collaboration]. Search for flavor-changing neutral currents in top quark decays  $t \rightarrow Hc$  and  $t \rightarrow Hu$  in multilepton final states in proton-proton collisions at  $\sqrt{s} = 13 \text{ TeV}$  with the ATLAS detector. *Phys. Rev. D* **2018**, *98*, 032002. [[CrossRef](#)]
59. Aaboud, M. et al. [ATLAS Collaboration]. Search for top quark decay  $t \rightarrow qH$ , with  $H \rightarrow \gamma\gamma$ , in  $\sqrt{s} = 13 \text{ TeV}$   $pp$  collisions using the ATLAS detector *JHEP* **2017**, *10*, 129. [[CrossRef](#)]
60. Aad, G. et al. [ATLAS Collaboration]. Search for flavour-changing neutral current top quark decays  $t \rightarrow Hq$  in  $pp$  collisions at  $\sqrt{s} = 8 \text{ TeV}$  with the ATLAS detector. *JHEP* **2015**, *12*, 61. [[CrossRef](#)]
61. Khachatryan, V. et al. [CMS Collaboration]. Search for top quark decays via Higgs-boson-mediated flavor-changing neutral currents in  $pp$  collisions at  $\sqrt{s} = 8 \text{ TeV}$ . *JHEP* **2017**, *2*, 79. [[CrossRef](#)]
62. Sirunyan, A. et al. [CMS Collaboration]. Search for the flavor-changing neutral current interactions of the top quark and the Higgs boson which decays into a pair of b quarks at  $\sqrt{s} = 13 \text{ TeV}$ . *JHEP* **2018**, *6*, 102. [[CrossRef](#)]
63. Tumasyan, A. et al. [CMS Collaboration]. Search for flavor-changing neutral current interactions of the top quark and Higgs boson in final states with two photons in proton-proton collisions at  $\sqrt{s} = 13 \text{ TeV}$ . *Phys. Rev. Lett.* **2022**, *129*, 032001. [[CrossRef](#)]
64. Tumasyan, A. et al. [CMS Collaboration]. Search for flavor-changing neutral current interactions of the top quark and the Higgs boson decaying to a bottom quark-antiquark pair at  $\sqrt{s} = 13 \text{ TeV}$ . *JHEP* **2022**, *2*, 169. [[CrossRef](#)]
65. Tumasyan, A. et al. [ATLAS Collaboration]. Search for flavour-changing neutral current interactions of the top quark and the Higgs boson in events with a pair of  $\tau$ -leptons in  $pp$  collisions at  $\sqrt{s} = 13 \text{ TeV}$  with the ATLAS detector. *arXiv* **2022**, arXiv:2208.11415.
66. LHC Higgs Cross Section Working Group. *Handbook of LHC Higgs Cross Sections: 4. Deciphering the Nature of the Higgs Sector*; CERN Yellow Reports: Geneva, Switzerland, 2017. [[CrossRef](#)]
67. Bevilacqua, G.; Worek, M. On the ratio of  $t\bar{b}b$  and  $t\bar{t}j$  cross sections at the CERN Large Hadron Collider. *JHEP* **2014**, *7*, 135. [[CrossRef](#)]
68. Aaboud, M. et al. [ATLAS Collaboration]. Measurements of fiducial and differential cross-sections of  $t\bar{t}$  production with additional heavy-flavour jets in proton-proton collisions at  $\sqrt{s} = 13 \text{ TeV}$  with the ATLAS detector. *JHEP* **2019**, *4*, 46. [[CrossRef](#)]
69. Sirunyan, A.M. et al. [CMS Collaboration]. Measurement of the cross section for  $t\bar{t}$  production with additional jets and b jets in  $pp$  collisions at  $\sqrt{s} = 13 \text{ TeV}$ . *JHEP* **2020**, *7*, 125. [[CrossRef](#)]
70. Sirunyan, A.M. et al. [CMS Collaboration]. Measurement of the  $t\bar{t}b\bar{b}$  production cross section in the all-jet final state in  $pp$  collisions at  $\sqrt{s} = 13 \text{ TeV}$ . *Phys. Lett. B* **2020**, *803*, 135285. [[CrossRef](#)]
71. Sirunyan, A.M. et al. [CMS Collaboration]. First measurement of the cross section for top quark pair production with additional charm jets using dileptonic final states in  $pp$  collisions at  $\sqrt{s} = 13 \text{ TeV}$ . *Phys. Lett. B* **2021**, *820*, 136565. [[CrossRef](#)]
72. Harnik, R.; Kopp, J.; Zupan, J. Flavor violating Higgs decays. *JHEP* **2013**, *3*, 26. [[CrossRef](#)]
73. Gorbahn, M.; Haisch, U. Searching for  $t \rightarrow c(u)h$  dipole moments. *JHEP* **2014**, *6*, 33. [[CrossRef](#)]
74. Larios, F.; Martinez, R.; Perez, M.A. Constraints on top quark FCNC from electroweak precision measurements. *Phys. Rev. D* **2005**, *72*, 057504. [[CrossRef](#)]
75. Fernandez, A.; Pagliarone, C.; Ramirez-Zavaleta, F.; Toscano, J.J. Higgs mediated double flavor violating top decays in effective theories. *J. Phys. G* **2010**, *37*, 085007. [[CrossRef](#)]
76. Hesari, H.; Khanpour, H.; Najafabadi, M. Direct and indirect searches for top-Higgs FCNC couplings. *Phys. Rev. D* **2015**, *92*, 113012. [[CrossRef](#)]
77. David, A. et al. [LHC Higgs Cross Section Working Group]. LHC HXSWG interim recommendations to explore the coupling structure of a Higgs-like particle. *arXiv* **2012**, arXiv:1209.0040.
78. Buchmuller, W.; Wyler, D. Effective lagrangian analysis of new interactions and flavour conservation. *Nucl. Phys. B* **1986**, *268*, 621. [[CrossRef](#)]
79. Grzadkowski, B.; Iskrzyński, M.; Misiak, M.; Rosiek, J. Dimension-six terms in the Standard Model Lagrangian. *JHEP* **2010**, *10*, 85. [[CrossRef](#)]
80. Aguilar-Saavedra, J.A.; Degrande, C.; Durieux, G.; Maltoni, F.; Vryonidou, E.; Zhang, C.; Barducci, D.; Brivio, I.; Cirigliano, V.; Dekens, W.; et al. Interpreting top-quark LHC measurements in the standard-model effective field theory. *arXiv* **2018**, arXiv:1802.07237.
81. Aguilar-Saavedra, J.A. A minimal set of top anomalous couplings. *Nucl. Phys. B* **2009**, *812*, 181. [[CrossRef](#)]
82. Aguilar-Saavedra, J.A. A minimal set of top-Higgs anomalous couplings. *Nucl. Phys. B* **2009**, *821*, 215. [[CrossRef](#)]
83. Degrande, C.; Maltoni, F.; Wang, J.; Zhang, C. Automatic computations at next-to-leading order in QCD for top-quark flavor-changing neutral processes. *Phys. Rev. D* **2015**, *91*, 034024. [[CrossRef](#)]
84. Durieux, G.; Maltoni, F.; Zhang, C. Global approach to top-quark flavor-changing interactions. *Phys. Rev. D* **2015**, *91*, 074017. [[CrossRef](#)]
85. Afik, Y.; Bar-Shalom, S.; Soni, A.; Wudka, J. New flavor physics in di- and tri-lepton events from single-top at the LHC and beyond. *Phys. Rev. D* **2021**, *103*, 075031. [[CrossRef](#)]

86. Barros, M.; Castro, N.F.; Erdmann, J.; Geßner, G.; Kröninger, K.; La Cagnina, S.; Peixoto, A. Study of interference effects in the search for flavour-changing neutral current interactions involving the top quark and a photon or a Z boson at the LHC. *Eur. Phys. J. Plus* **2020**, *135*, 339. [[CrossRef](#)]
87. Sirunyan, A.M. et al. [CMS Collaboration]. Search for new physics in top quark production in dilepton final states in proton-proton collisions at  $\sqrt{s} = 13$  TeV. *Eur. Phys. J. C* **2019**, *79*, 886. [[CrossRef](#)]
88. Bardhan, D.; Bhattacharyya, G.; Ghosh, D.; Patra, M.; Raychaudhuri, S. A detailed analysis of flavour-changing decays of top quarks as a probe of new physics at the LHC. *Phys. Rev. D* **2016**, *94*, 015026. [[CrossRef](#)]
89. Branco, G.C.; Ferreira, P.M.; Lavoura, L.; Rebelo, M.N.; Sher, M.; Silva J.P. Theory and phenomenology of two-Higgs-doublet-models. *Phys. Rept.* **2012**, *516*, 1. [[CrossRef](#)]
90. Gunion, J.F.; Haber, H.E. CP-conserving two-Higgs-doublet-model: The approach of the decoupling limit. *Phys. Rev. D* **2003**, *67*, 075019. [[CrossRef](#)]
91. Maiani, L.; Polosa, A.D.; Riquer, V. Bounds to the Higgs sector masses in minimal supersymmetry from LHC data. *Phys. Lett. B* **2013**, *724*, 274. [[CrossRef](#)]
92. Hou, W.-S. Tree level  $t \rightarrow ch$  or  $h \rightarrow t\bar{c}$  decays. *Phys. Lett. B* **1992**, *296*, 179. [[CrossRef](#)]
93. Sirunyan, A. et al. [CMS Collaboration]. Combined measurement of Higgs boson couplings in proton-proton collisions at  $\sqrt{s} = 13$  TeV. *Eur. Phys. J. C* **2019**, *79*, 421. [[CrossRef](#)] [[PubMed](#)]
94. Aaboud, M. et al. [ATLAS Collaboration]. Combined measurements of Higgs boson production and decay using up to 80  $fb^{-1}$  of proton-proton collision data at  $\sqrt{s} = 13$  TeV collected with the ATLAS experiment. *Phys. Rev. D* **2020**, *101*, 012002. [[CrossRef](#)]
95. Aaboud, M. et al. [ATLAS Collaboration]. Search for heavy resonances decaying into  $WW$  in  $ev\mu\nu$  final state in pp collisions at  $\sqrt{s} = 13$  TeV with the ATLAS detector. *Eur. Phys. J. C* **2018**, *78*, 24. [[CrossRef](#)] [[PubMed](#)]
96. Pich, A.; Tuzon, P. Yukawa alignment in the two-higgs-doublet model. *Phys. Rev. D* **2009**, *80*, 091702. [[CrossRef](#)]
97. Abbas, G.; Celis, A.; Li, X.-Q.; Lu, J.; Pich, A. Flavour-changing top decays in the aligned two-Higgs-doublet model. *JHEP* **2015**, *6*, 005. [[CrossRef](#)]
98. Das, A. K.; Kao, C. A two Higgs doublet model for the top quark. *Phys. Lett. B* **1996**, *372*, 106. [[CrossRef](#)]
99. Kao, C.; Cheng, H.-I.; Hou, W.-S.; Sayre, J. Top decays with flavor changing neutral Higgs interactions at the LHC. *Phys. Lett. B* **2012**, *716*, 225. [[CrossRef](#)]
100. Chen, K.-F.; Hou, W.-S.; Kao, C.; Kohda, M. When the Higgs meets the Top: Search for  $t \rightarrow ch^0$  at the LHC. *Phys. Lett. B* **2013**, *725*, 378. [[CrossRef](#)]
101. Jain, R.; Kao, C. Charming top decays with flavor changing neutral Higgs boson and  $WW$  at hadron colliders. *Phys. Rev. D* **2019**, *99*, 055036. [[CrossRef](#)]
102. Baum, I.; Eilam, G.; Bar-Shalom, S. Scalar flavor changing neutral currents and rare top quark decays in a two Higgs doublet model “for the top quark”. *Phys. Rev. D* **2008**, *77*, 113008. [[CrossRef](#)]
103. Branco, G.; Grimus, W.; Lavoura, L. Relating the scalar flavor changing neutral couplings to the CKM matrix. *Phys. Lett. B* **1996**, *380*, 119. [[CrossRef](#)]
104. Botella, F.; Branco, G.; Rebelo, M. Minimal flavour violation and multi-Higgs models. *Phys. Lett. B* **2010**, *687*, 194. [[CrossRef](#)]
105. Botella, F.; Branco, G.; Nebot, M.; Rebelo, M. Flavour-changing Higgs couplings in a class of two Higgs doublet models. *Eur. Phys. J. C* **2016**, *76*, 161. [[CrossRef](#)]
106. Djouadi, A. The anatomy of electroweak symmetry breaking Tome II: The Higgs bosons in the Minimal Supersymmetric Model. *Phys. Rept.* **2008**, *459*, 1. [[CrossRef](#)]
107. Fayet, P. Supersymmetry and weak, electromagnetic, and strong interactions. *Phys. Lett. B* **1976**, *64*, 159. [[CrossRef](#)]
108. Fayet, P. Spontaneously broken supersymmetric theories of weak, electromagnetic, and strong interactions. *Phys. Lett. B* **1977**, *69*, 489. [[CrossRef](#)]
109. Djouadi, A.; Maiani, L.; Moreau, G.; Polosa, A.; Quevillon, J.; Riquer, V. The post-Higgs MSSM scenario: Habemus MSSM? *Eur. Phys. J. C* **2013**, *73*, 2650. [[CrossRef](#)]
110. Djouadi, A.; Maiani, L.; Polosa, A.; Quevillon, J.; Riquer, V. Fully covering the MSSM Higgs sector at the LHC. *JHEP* **2015**, *6*, 168. [[CrossRef](#)]
111. Dedes, A.; Paraskevas, M.; Rosiek, J.; Suxho, K.; Tamvakis, K. Rare top-quark decays to Higgs boson in MSSM. *JHEP* **2014**, *11*, 137. [[CrossRef](#)]
112. Eilam, G.; Gemintern, A.; Han, T.; Yang, J. M.; Zhang, X. Top-quark rare decay  $t \rightarrow ch$  in R-parity-violating SUSY. *Phys. Lett. B* **2001**, *510*, 227. [[CrossRef](#)]
113. Perez, P.F.; Wise, M.B. Baryon and lepton number as local gauge symmetries. *Phys. Rev. D* **2010**, *82*, 011901. [[CrossRef](#)]
114. Perez, P.F.; Wise, M.B. Low energy supersymmetry with baryon and lepton number gauged. *Phys. Rev. D* **2011**, *84*, 055015. [[CrossRef](#)]
115. Perez, P.F.; Wise, M.B. Breaking local baryon and lepton number at the TeV scale. *JHEP* **2011**, *8*, 68. [[CrossRef](#)]
116. Amond, J.M.; Perez, P.F.; Formal, B.; Spinner, S. Higgs boson decays, baryon number violation, and supersymmetry at the LHC. *Phys. Rev. D* **2012**, *85*, 115024. [[CrossRef](#)]
117. Gao, T.-J.; Feng, T.-F.; Sun, F.; Zhang, H.-B.; Zhao, S.-M. Top quark decay to a 125 GeV Higgs in BLMSSM. *Chin. Phys. C* **2015**, *39*, 073101. [[CrossRef](#)]

118. Ellwanger, U.; Hugonie, C.; Teixeira, A. M. The Next-to-Minimal Supersymmetric Standard Model. *Phys. Rept.* **2010**, *496*, 1. [[CrossRef](#)]
119. Kim, J.E.; Nilles, H.P. The  $\mu$ -problem and the strong CP-problem. *Phys. Lett. B* **1984**, *138*, 150. [[CrossRef](#)]
120. Del Aguila, F.; Aguilar-Saavedra, J.A.; Miquel, R. Constraints on top couplings in models with exotic quarks. *Phys. Rev. Lett.* **1999**, *82*, 1628. [[CrossRef](#)]
121. Gaitan, R.; Miranda, O.; Gabral-Rosetti, L. Rare top quark and Higgs boson decays in alternative left-right symmetric models. *Phys. Rev. D* **2005**, *72*, 034018. [[CrossRef](#)]
122. Yang, B.; Liu, N.; Han, J. Top quark flavour-changing neutral-current decay to a 125 GeV Higgs boson in the littlest Higgs model with T parity. *Phys. Rev. D* **2014**, *89*, 034020. [[CrossRef](#)]
123. Azatov, A.; Toharia, M.; Zhu, L. Higgs mediated flavor changing neutral currents in warped extra dimensions. *Phys. Rev. D* **2009**, *80*, 035016. [[CrossRef](#)]
124. Casagrande, S.; Goertz, F.; Haisch, U.; Neubert, M.; Pfoh, T. The custodial Randall-Sundrum model: From precision tests to Higgs physics. *JHEP* **2010**, *9*, 14. [[CrossRef](#)]
125. Dey, U.K.; Jha, T. Rare top decays in Minimal and Non-minimal Universal Extra Dimension. *Phys. Rev. D* **2016**, *94*, 056011. [[CrossRef](#)]
126. Dimopoulos, S.; Preskill, J. Massless composites with massive constituents. *Nucl. Phys. B* **1982**, *199*, 206. [[CrossRef](#)]
127. Kaplan, D.B.; Georgi, H. SU(2) x U(1) breaking by vacuum misalignment. *Phys. Lett. B* **1984**, *136*, 183. [[CrossRef](#)]
128. Kaplan, D.B.; Georgi, H.; Dimopoulos, S. Composite Higgs scalars. *Phys. Lett. B* **1984**, *136*, 187. [[CrossRef](#)]
129. Cacciapaglia, G.; Ferretti, G.; Flacke, T.; Serodio, H. Light scalars in composite Higgs models. *Front. Phys.* **2019**, *7*, 22. [[CrossRef](#)]
130. Castro, N.; Chala, M.; Peixoto, A.; Ramos, M. Novel flavour-changing neutral currents in the top quark sector. *JHEP* **2020**, *10*, 38. [[CrossRef](#)]
131. Banerjee, S.; Chala, M.; Spannowsky, M. Top quark FCNCs in extended Higgs sectors. *Eur. Phys. J. C* **2018**, *78*, 683. [[CrossRef](#)]
132. Kaplan, D. Flavor at SSC energies: A new mechanism for dynamically generated fermion masses. *Nucl. Phys. B* **1991**, *365*, 259. [[CrossRef](#)]
133. Altunkaynak, B.; Hou, W.-S.; Kao, C.; Kohda, M.; McCoy, B. Flavor changing heavy Higgs interactions at the LHC. *Phys. Lett. B* **2015**, *751*, 135. [[CrossRef](#)]
134. Hou, W.-S.; Modak, T. Probing top changing neutral Higgs couplings at colliders. *Mod. Phys. Lett. A* **2021**, *36*, 2130006. [[CrossRef](#)]
135. Kohda, M.; Modak, T.; Hou, W.-S. Searching for new scalar bosons via triple-top signature in  $cg \rightarrow tS^0 \rightarrow t\bar{t}$ . *Phys. Lett. B* **2018**, *776*, 379. [[CrossRef](#)]
136. Hou, W.-S.; Kohda, M.; Modak, T. Constraining a lighter exotic scalar via same-sign top. *Phys. Lett. B* **2018**, *786*, 212. [[CrossRef](#)]
137. Hou, W.-S.; Hsu T.-H.; Modak, T. Constraining  $t \rightarrow u$  flavor changing neutral Higgs coupling at the LHC. *Phys. Rev. D* **2020**, *102*, 055006. [[CrossRef](#)]
138. Gori, S.; Grojean, C.; Juste, A.; Paul, A. Heavy Higgs searches: Flavour matters. *JHEP* **2018**, *1*, 108. [[CrossRef](#)]
139. Knapen, S.; Robinson, D.J. Disentangling mass and mixing hierarchies. *Phys. Rev. Lett.* **2015**, *115*, 161803. [[CrossRef](#)]
140. Altmannshofer, W.; Gori, S.; Robinson, D.J.; Tuckler, D. The Flavor-locked Flavorful Two Higgs Doublet Model. *JHEP* **2018**, *3*, 129. [[CrossRef](#)]
141. Altmannshofer, W.; Eby, J.; Gori, S.; Lotito, M.; Martone, M.; Tuckler, D. Collider signatures of flavorful Higgs bosons. *Phys. Rev. D* **2016**, *94*, 115032. [[CrossRef](#)]
142. Altmannshofer, W.; Maddock, B.; Tuckler, D. Rare top decays as probes of flavorful Higgs bosons. *Phys. Rev. D* **2019**, *100*, 015003. [[CrossRef](#)]
143. Arroyo-Urena, M.A.; Fernandez-Tellez, A.; Tavares-Velasco, G. Flavor changing Flavon decay  $\phi \rightarrow tc$  ( $\phi = H_F, A_F$ ) at the high-luminosity large hadron collider. *arXiv* **2019**, arXiv:1906.07821.
144. FCC Collaboration. FCC Physics Opportunities: Future Circular Collider Conceptual Design Report Volume 1. *Eur. Phys. J. C* **2019**, *79*, 474. [[CrossRef](#)]
145. Fernandez, J.L.A. et al. [LHeC Collaboration]. A Large Hadron Electron Collider at CERN: Report on the physics and design concepts for machine and detector. *J. Phys. G Nucl. Part. Phys.* **2012**, *39*, 075001. [[CrossRef](#)]
146. Bruening, O.; Klein, M. The Large Hadron Electron Collider. *Mod. Phys. Lett. A* **2013**, *28*, 1330011. [[CrossRef](#)]
147. Klein, M. *From My Vast Repertoire . . . : Guido Altarelli's Legacy*; Forte, S., Aharon, L., Ridolfi, G., Eds.; World Scientific Publishing: Singapore, 2018. [[CrossRef](#)]
148. Klein, M. Deep inelastic scattering at the energy frontier. *Ann. Der Phys.* **2016**, *528*, 138. [[CrossRef](#)]
149. Turk Cakir, I.; Yilmaz, A.; Denizli, H.; Senol, A.; Karadeniz, H.; Cakir, O. Probing the anomalous FCNC couplings at Large Hadron Electron Collider. *Adv. High Energy Phys.* **2017**, *2017*, 1572053. [[CrossRef](#)]
150. Behera, S.; Islam, R.; Kumar, M.; Poulouse, P.; Rahaman, R. Fingerprinting the top quark FCNC via anomalous  $Ztq$  couplings at the LHeC. *Phys. Rev. D* **2019**, *100*, 015006. [[CrossRef](#)]
151. Cakir, O.; Yilmaz, A.; Turk Cakir, I.; Senol, A.; Denizli, H. Probing top quark FCNC  $tq\gamma$  and  $tqZ$  couplings at future electron-proton colliders. *Nucl. Phys. B* **2019**, *944*, 114640. [[CrossRef](#)]
152. Wang, X.; Sun, H.; Luo, X. Searches for the anomalous FCNC top-Higgs couplings with polarized electron beam at the LHeC. *Adv. High Energy Phys.* **2017**, *2017*, 4693213. [[CrossRef](#)]

153. Bordry, F.; Benedikt, M.; Bruning, O.; Jowett, J.; Rossi, L.; Schulte, D.; Stapnes, S.; Zimmermann, F. Machine parameters and projected luminosity performance of proposed future colliders at CERN. *arXiv* **2018**, arXiv:1810.13022.
154. Bruning, O.; Jowett, J.; Klein, M.; Pellegrini, D.; Schulte, D.; Zimmermann, F. *Future Circular Collider Study FCC-he Baseline Parameters*; Technical Report; CERN: Meyrin, Switzerland, 2018.
155. Behera, S.; Poulou, P. Tracing the anomalous  $tqg$  and  $tq\gamma$  flavor changing interactions at the FCC-he. *arXiv* **2020**, arXiv:2007.02236.
156. FCC Collaboration. FCC-ee: The Lepton Collider: Future Circular Collider Conceptual Design Report Volume 2. *Eur. Phys. J. ST* **2019**, *228*, 261. [[CrossRef](#)]
157. FCC Collaboration. FCC-hh: The Hadron Collider: Future Circular Collider Conceptual Design Report Volume 3. *Eur. Phys. J. ST* **2019**, *228*, 755. [[CrossRef](#)]
158. Mandrik, P. et al. [the FCC Study Group]. Prospect for top quark FCNC searches at the FCC-hh. *J. Phys. Conf. Ser.* **2019**, *1390*, 012044. [[CrossRef](#)]
159. Papaefstathiou, A.; Tetlalmatzi-Xolocotzi G. Rare top quark decays at a 100 TeV proton-proton collider:  $t \rightarrow bWZ$  and  $t \rightarrow hc$ . *Eur. Phys. J. C* **2018**, *78*, 214. [[CrossRef](#)]
160. Oyulmaz, K.Y.; Senol, A.; Denizli, H.; Cakir, O. Top quark anomalous FCNC production via  $tqg$  couplings at FCC-hh. *Phys. Rev. D* **2019**, *99*, 115023. [[CrossRef](#)]
161. Oyulmaz, K.Y.; Senol, A.; Denizli, H.; Yilmaz, A.; Turk Cakir, I.; Cakir, O. Probing anomalous  $tq\gamma$  and  $tqg$  couplings via single top production in association with photon at FCC-hh. *Eur. Phys. J. C* **2019**, *79*, 83. [[CrossRef](#)]
162. Abada, A. et al. [FCC Collaboration]. Future Circular Collider Study: Vol. 4 The High-Energy LHC (HE-LHC). *Eur. Phys. J. Spec. Top.* **2019**, *228*, 1109. [[CrossRef](#)]
163. Liu, Y.-B.; Moretti, S. Probing the top-Higgs boson FCNC couplings via the  $h \rightarrow \gamma\gamma$  channel at the HE-LHC and FCC-hh. *Phys. Rev. D* **2020**, *101*, 075029. [[CrossRef](#)]
164. Moortgat-Pick, G.; Abe, T.; Alexander, G.; Ananthanarayan, B.; Babich, A.A.; Bharadwaj, V.; Barber, D.; Bartl, A.; Brachmann, A.; Chen, S. The role of polarized positrons and electrons in revealing fundamental interactions at the Linear Collider. *Phys. Rept.* **2008**, *460*, 131. [[CrossRef](#)]
165. Zarnecki, A. Sensitivity of CLIC at 380 GeV to the top FCNC decay  $t \rightarrow cH$ . *J. Phys. Conf. Ser.* **2017**, *873*, 012049. [[CrossRef](#)]
166. Zarnecki, A. Top-quark physics at the first CLIC stage. *arXiv* **2018**, arXiv:1810.05487.
167. Abramowicz, H. et al. [CLICdp Collaboration]. Top-quark physics at the CLIC electron-positron linear collider. *JHEP* **2019**, *11*, 003. [[CrossRef](#)]
168. Melic, B.; Patra, M. Exploring the top-Higgs FCNC couplings at polarized linear colliders with top spin observables. *JHEP* **2017**, *01*, 048. [[CrossRef](#)]